Anal. Chem. **2010,** *82,* 2753–2758

Atmospheric Pressure Femtosecond Laser Imaging Mass Spectrometry

Yves Coello,[†] A. Daniel Jones,[†,‡] Tissa C. Gunaratne,[§] and Marcos Dantus*[,†,||]

Department of Chemistry, Department of Biochemistry and Molecular Biology, Department of Physics, Michigan State University, East Lansing, Michigan 48824, and BioPhotonic Solutions Inc., Okemos, Michigan 48864

A novel atmospheric pressure imaging mass spectrometry approach that offers improved lateral resolution (10 μm) using near-infrared femtosecond laser pulses for nonresonant desorption and ionization of sample constituents without the need of a laser-absorbing matrix is demonstrated. As a proof of concept the method was used to image a two-chemical pattern in paper. To demonstrate the ability of the approach to analyze biological tissue, a monolayer of onion epidermis was imaged allowing the chemical visualization of individual cells using mass spectrometry at ambient conditions for the first time. As the spatial resolution is currently limited by the limit of detection of the setup (~500 fmol limit of detection for citric acid), improvements in sensitivity will increase the achievable spatial resolution.

Imaging mass spectrometry (IMS)[1,2] has become an important tool in the life sciences because of its ability to localize specific analytes, from small metabolites to proteins, in biological samples. There are two different ways to obtain the spatial information in an IMS experiment. Typically a tightly focused ionization beam is used to examine a small region of the sample from where a mass spectrum is obtained. This process is repeated until the whole sample area has been analyzed and a mass spectrum for each position has been stored. Chemical images can then be obtained from the set of mass spectra and the corresponding spatial coordinates. This approach, called microprobe mode, requires the sample to be probed point by point and therefore is relatively slow because it is limited by the rate of data acquisition and/or repetition rate of the laser beam. In addition, the spatial resolution is limited by the size of the focused ionization beam. Although much less popular than the microprobe mode a powerful approach that overcomes the previous limitations has been demonstrated. In the microscope mode[3,4] the tightly focused ionization beam is replaced by one that illuminates a relatively large area of the sample (~200 μm), and ion detection is spatially resolved. However, the microscope mode can only be applied in vacuum conditions to preserve the ion trajectories from multiple locations in the sample to the detector.

Secondary ion mass spectrometry (SIMS)[5,6] and matrix-assisted laser desorption/ionization (MALDI)[7,8] are currently the most popular techniques used for obtaining chemically resolved images. In SIMS a beam of primary ions is used to bombard the sample surface and generate secondary ions. SIMS provides the highest spatial resolution available (typically >50 nm), however it has only proved useful for identifying elements and low mass molecules (ca. < 1000 Da) because the ionization method leads to fragmentation that is more pronounced for higher mass analytes. SIMS requires vacuum conditions and is therefore, incompatible with the analysis of live cells and tissues. To analyze the distribution of macromolecules such as proteins ($1000 < m/z < 50\,000$), ultraviolet (UV) MALDI remains the method of choice. This technique requires treating the sample with an external matrix that absorbs the radiation, which makes sample preparation a critical step. Most UV MALDI imaging experiments have been performed under vacuum conditions providing typical spatial resolutions of 25−200 μm as limited by laser spot size and perturbation of analyte localization during matrix addition. Several atmospheric pressure (AP) ionization techniques have been developed in the past years to overcome incompatibility with the analysis of live tissues and other limitations imposed by a vacuum environment.[9] Some of these AP ionization techniques, laser ablation inductively coupled plasma (LA-ICP),[10,11] laser ablation electrospray ionization (LAESI),[12,13] infrared (IR) MALDI,[14,15] and desorption electrospray ionization (DESI)[16,17] have already been applied to IMS. In contrast to the rest of these methods, LA-ICP does not provide molecular information and can only be used for

* To whom correspondence should be addressed. E-mail: dantus@msu.edu.
† Department of Chemistry.
‡ Department of Biochemistry and Molecular Biology.
§ BioPhotonic Solutions Inc.
|| Department of Physics.

(1) Heeren, R. M. A.; Smith, D. F.; Stauber, J.; Kukrer-Kaletas, B.; MacAleese, L. *J. Am. Soc. Mass Spectrom.* **2009**, *20*, 1006–1014.
(2) McDonnell, L. A.; Heeren, R. M. A. *Mass Spec. Rev.* **2007**, *26*, 606–643.
(3) Luxembourg, S. L.; Mize, T. H.; McDonnell, L. A.; Heeren, R. M. A. *Anal. Chem.* **2004**, *76*, 5339–5344.
(4) Luxembourg, S. L.; McDonnell, L. A.; Mize, T. H.; Heeren, R. M. A. *J. Proteome Res.* **2005**, *4*, 671–673.
(5) Boxer, S. G.; Kraft, M. L.; Weber, P. K. *Annu. Rev. Biophys.* **2009**, *38*, 53–74.
(6) Winograd, N. *Anal. Chem.* **2005**, *77*, 142A–149A.
(7) Franck, J.; Arafah, K.; Elayed, M.; Bonnel, D.; Vergara, D.; Jacquet, A.; Vinatier, D.; Wisztorski, M.; Day, R.; Fournier, I.; Salzet, M. *Mol. Cell. Proteomics* **2009**, *8*, 2023–2033.
(8) Cornett, D. S.; Reyzer, M. L.; Chaurand, P.; Caprioli, R. M. *Nat. Methods* **2007**, *4*, 828–833.
(9) Van Berkel, G. J.; Pasilis, S. P.; Ovchinnikova, O. *J. Mass Spectrom.* **2008**, *43*, 1161–1180.
(10) Becker, J. S.; Zoriy, M. V.; Pickhardt, C.; Palomero-Gallagher, N.; Zilles, K. *Anal. Chem.* **2005**, *77*, 3208–3216.
(11) Wu, B.; Zoriy, M.; Chen, Y. X.; Becker, J. S. *Talanta* **2009**, *78*, 132–137.
(12) Nemes, P.; Vertes, A. *Anal. Chem.* **2007**, *79*, 8098–8106.
(13) Nemes, P.; Barton, A. A.; Vertes, A. *Anal. Chem.* **2009**, *81*, 6668–6675.
(14) Li, Y.; Shrestha, B.; Vertes, A. *Anal. Chem.* **2007**, *79*, 523–532.
(15) Li, Y.; Shrestha, B.; Vertes, A. *Anal. Chem.* **2008**, *80*, 407–420.
(16) Wiseman, J. M.; Ifa, D. R.; Song, Q. Y.; Cooks, R. G. *Angew. Chem., Int. Ed.* **2006**, *45*, 7188–7192.

10.1021/ac9026466
Published on Web 03/08/2010

elemental analysis of the sample because ICP is an atomic ion source. IR MALDI has employed a 2940 nm wavelength laser for both desorption and ionization of chemicals using the inherent water content present in biological samples as a matrix. LA-ICP and LAESI use a laser to ablate the sample while a postionization method, ICP and electrospray ionization (ESI) respectively, is employed to generate the ions. In LAESI the use of a postionization process following laser desorption (ablation) leads to higher ionization efficiencies compared to IR MALDI because laser ablation typically produces a significant proportion of neutral species in addition to ions and clusters. Although ink mock patterns have been analyzed with 40 μm spatial resolution using AP IR MALDI[14] and DESI,[18] imaging biological samples at AP with a spatial resolution better than ~200 μm has not been reported yet. A higher spatial resolution would be desirable, as it would allow studying, for instance, the distribution of chemicals in cellular and subcellular structures.

The spatial resolution of a laser ablation IMS experiment depends on the laser spot size and the step size,[2] which is the distance the laser focal spot moves to analyze an adjacent sample location. Typically, the step size is larger than the laser spot and thus is the limiting factor in determining the lateral resolution of the imaging experiment. However, a step size smaller than the laser spot can be used in an approach known as oversampling.[19] This method requires complete removal of the analyte within the laser ablation volume by the desorption process or the use of data processing algorithms. With oversampling the step size becomes the limiting factor in determining the spatial resolution and is itself referred to as the pixel resolution of the experiment. In this situation, decreasing the step size leads to a higher spatial resolution but also to a smaller sampled volume and thus to lower signal. Using oversampling, an AP IR-MALDI chemical image of a dye mock pattern with 40 μm resolution has been demonstrated.[14] Recently, significant progress toward chemical imaging with cellular resolution has been reported using LAESI.[20] This experiment demonstrated in situ metabolic profiling of single large cells (~50 μm width) with a 2940 nm laser beam coupled to a glass fiber. However, no actual chemical image was presented.

Near IR (NIR) femtosecond laser pulses coupled with mass spectrometry have been used to demonstrate improved gas-phase molecular identification, including isomer differentiation,[21,22] and laser-controlled molecular fragmentation.[23] More recently, femtosecond-laser induced ionization/dissociation (fs-LID) of protonated peptides has been shown to provide greater sequence information than conventional ion activation methods.[24] Femtosecond laser pulses have also been used for ablation with ion-trap MS,[25] LA-ICP,[26] ESI,,[27] and as a postionization method for molecular imaging after ion beam desorption[28] and laser ablation[29] of molecular thin films. MALDI experiments using femtosecond laser pulses in different wavelength regions have showed very similar results to those using nanosecond pulsed lasers.[30] NIR femtosecond laser (800 nm) MALDI mass spectra using standard matrices with absorption bands in the UV spectrum have been recently demonstrated.[31] However, due to the very high peak power densities achieved by focused femtosecond laser pulses (~10^{14} W/cm^2) direct nonresonant ablation and ionization of the analytes can occur.[32] Here we use such an approach for IMS at AP conditions. Focused NIR femtosecond laser pulses are used to ablate and ionize the sample without using a laser-absorbing matrix, either native or external, making sample preparation and handling significantly simpler. Due to its AP implementation the method is a promising imaging technique for in vivo studies. Finally, the spatial resolution provided by our AP femtosecond laser desorption ionization (fs-LDI) IMS approach is significantly higher than that of other AP IMS techniques. Here we demonstrate 10 μm spatial resolution in a biological tissue sample (onion epidermis monolayer) allowing the chemical visualization of individual cells using mass spectrometry under atmospheric pressure conditions for the first time.

EXPERIMENTAL SECTION

Mass Spectrometer and Laser System. Femtosecond laser pulses from a Ti:Sapphire oscillator (Micra, Coherent) were shaped by a multiphoton intrapulse interference phase scan[33] (MIIPS, BioPhotonic Solutions Inc.) enabled pulse shaper containing a 128-pixel spatial light modulator (SLM, CRi) and amplified by a regenerative amplifier (Legend USP, Coherent). The output pulses (1 kHz, centered at 800 nm) were focused on the sample using a 5× objective. For the "S" character, onion tissue and limit of detection experiments 3, 15, and 3 μJ pulses were used, respectively. The focused laser pulses had a spot diameter of ~20 μm, determined from the optical image of the ablation craters produced by the laser on the onion epidermis tissue. The ion source of a time-of-flight mass spectrometer (Micromass LCT, Waters) was replaced with a custom-made AP femtosecond laser ion source containing a motorized XY stage (MAX200, Thorlabs) which holds the sample ~5 mm from the sample cone of the mass spectrometer. For the "S" character and limit of detection experiments a copper surface with a −200 V DC offset was used

(17) Wiseman, J. M.; Ifa, D. R.; Zhu, Y. X.; Kissinger, C. B.; Manicke, N. E.; Kissinger, P. T.; Cooks, R. G. *Proc. Natl. Acad. Sci. U.S.A.* **2008**, *105*, 18120–18125.
(18) Kertesz, V.; Van Berkel, G. J. *Rapid Commun. Mass Spectrom.* **2008**, *22*, 2639–2644.
(19) Jurchen, J. C.; Rubakhin, S. S.; Sweedler, J. V. *J. Am. Soc. Mass Spectrom.* **2005**, *16*, 1654–1659.
(20) Shrestha, B.; Vertes, A. *Anal. Chem.* **2009**, *81*, 8265–8271.
(21) Pastirk, I.; Zhu, X.; Lozovoy, V. V.; Dantus, M. *Appl. Opt.* **2007**, *46*, 4041–4045.
(22) Dela Cruz, J. M.; Lozovoy, V. V.; Dantus, M. *J. Mass Spectrom.* **2007**, *42*, 178–186.
(23) Lozovoy, V. V.; Zhu, X.; Gunaratne, T. C.; Harris, D. A.; Shane, J. C.; Dantus, M. *J. Phys. Chem. A* **2008**, *112*, 3789–3812.
(24) Kalcic, C. L.; Gunaratne, T. C.; Jones, A. D.; Dantus, M.; Reid, G. E. *J. Am. Chem. Soc.* **2009**, *131*, 940–942.
(25) Samek, O.; Margetic, V.; von Wiren, N.; Michels, A.; Niemax, K.; Hergenroder, R. *Appl. Phys. A: Mater. Sci. Process.* **2004**, *79*, 957–960.
(26) Fernandez, B.; Claverie, F.; Pecheyran, C.; Donard, O. F. X. *Trends Anal. Chem.* **2007**, *26*, 951–966.
(27) Brady, J. J.; Judge, E. J.; Levis, R. J. *Rapid Commun. Mass Spectrom.* **2009**, *23*, 3151–3157.
(28) Willingham, D.; Kucher, A.; Winograd, N. *Chem. Phys. Lett.* **2009**, *468*, 264–269.
(29) Savina, M. R.; Lykke, K. R. *Anal. Chem.* **1997**, *69*, 3741–3746.
(30) Papantonakis, M. R.; Kim, J.; Hess, W. P.; Haglund, R. F. *J. Mass Spectrom.* **2002**, *37*, 639–647.
(31) Wichmann, J. M.; Lupulescu, C.; Woste, L.; Lindinger, A. *Rapid Commun. Mass Spectrom.* **2009**, *23*, 1105–1108.
(32) Gamaly, E. G.; Rode, A. V.; Luther-Davies, B.; Tikhonchuk, V. T. *Phys. Plasmas* **2002**, *9*, 949–957.
(33) Coello, Y.; Lozovoy, V. V.; Gunaratne, T. C.; Xu, B. W.; Borukhovich, I.; Tseng, C. H.; Weinacht, T.; Dantus, M. *J. Opt. Soc. Am. B* **2008**, *25*, A140–A150.

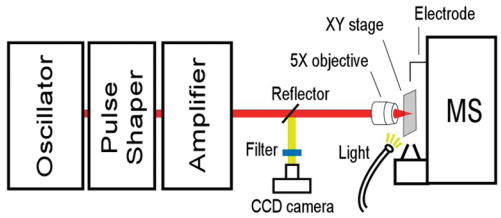

Figure 1. Atmospheric pressure femtosecond laser desorption ionization imaging mass spectrometry (AP fs-LDI IMS) setup. Femtosecond laser pulses from a Ti:Sapphire oscillator were regeneratively amplified and focused on the sample by a 5× objective. The pulse shaper was used to compress the pulses at the focus. The sample was placed on a motorized XY stage close to the sample cone of the mass spectrometer (MS) and a counter-electrode was used to direct the ions to the sample cone. To obtain the optical images the light illuminating the sample was collected by the objective and directed to a CCD camera. A filter before the camera was used to block the scattered laser light.

as a sample holder. For the onion tissue experiments the sample was free-standing, only held to the XY stage from the upper edge. For all the experiments, the sample was positioned between the sample cone (±65 V DC) and a repeller electrode (±1 kV DC) so that the potential difference helped to direct the ion plume toward the inlet (Figure 1), where the + and − signs apply for positive and negative ion mode experiments, respectively. The mass scale was calibrated periodically using MassLynx 4.1 software (Waters Corp.) and electrospray ionization of a commercial NaCsI solution (Waters Corp.). The accuracy of measured m/z values was better than 100 mDa over the studied range ($m/z < 500$) over multiple days between calibrations.

Femtosecond laser pulses shorter than ~50 fs are prone to temporal broadening when they travel through optical media (lenses, objectives, and even air) owing to their broad spectral bandwidth. A way to compress the pulses at the position of the target is necessary to achieve optimal and reproducible results. In our experiments, the main optical element broadening the pulses is the 5× objective. We use MIIPS[33] to compress the pulses after the objective, to obtain transform-limited 45 fs pulses at the focal plane, the shortest possible duration for the available bandwidth. This process of pulse compression is of critical importance to ensure efficient and reproducible ablation and ionization within the focal volume.

Imaging. The motorized stage was computer-controlled to move the sample surface laterally. Mass spectra were averaged for ~2 s for every spot on the sample and were stored as a function of time. Data acquisition for each imaging experiment took ~80 min. A computer program then converted spectrum acquisition time to the corresponding spatial coordinates. Finally, chemical images were obtained by plotting two-dimensional distributions of the different chemical species. To obtain the optical images, the sample was illuminated with a USB-powered diode and the light collected by the objective was reflected by an 800 nm-transmitter/400 nm-reflector and directed to a monochromatic CCD camera (Apogee Alta, Apogee Instruments, Inc.). A BG40 filter was placed before the CCD camera to block the remaining scattered laser light (Figure 1).

Materials and Sample Preparation. All solutions were prepared in deionized water. Citric acid (monohydrate) was purchased from J.T. Baker. The iodide/iodine dye solution was prepared by dissolving 10 mg of iodine and 175 mg of potassium iodide (Mallinckrodt) in 1 mL of water. For the "S" experiment the handwritten marks were produced on bond paper using a 0.25 mm diameter wire. The paper sample was then glued to the copper sample holder and transferred to the translation stage. Fresh red onions were purchased from a local supermarket. Onion epidermis tissue sections were obtained with a razor blade, transferred to the translation stage and analyzed without any pretreatment. In the partially stained tissue experiment, iodine/iodide dye was deposited on a region of an onion tissue section by a 0.25 mm diameter wire before transferring the sample to the translation stage. For the limit of detection experiment, 1 μL of an aqueous 10 mM solution of citric acid was deposited on the copper sample holder and the solution was allowed to dry under ambient conditions. The deposited material covered an area of ~6 mm^2.

Metabolite Identification. Confirmations of metabolite annotation were performed on extracts (methanol:water, 1:1 v/v) of onion tissue (1.0 mL of solvent per 100 mg of tissue, wet weight) using an LCT Premier (Waters) mass spectrometer that was coupled to a Shimadzu LC-20AD ternary pump. Extracts were analyzed using negative mode ESI following separation on an Ascentis Express C18 column (2.1 × 50 mm, Supelco) using a gradient described previously.[34] Accurate mass assignments were aided by use of a lock mass reference (*N*-butylbenzenesulfonamide) and comparisons of retention times and ion masses to authentic standards (Sigma-Aldrich).

RESULTS AND DISCUSSION

The motivation for developing improved IMS instrumentation is to obtain chemical-species resolved images. In order to demonstrate this capability we analyzed an "S" character drawn with iodide/iodine dye. An optical image of the sample is shown in Figure 2a. Also present, although not visible in the optical image, is a diagonal mark across the "S" character produced with an aqueous ~5% (w/v) solution of citric acid. The mass spectrum of the dye showed the presence of peaks at m/z 126.91, 253.77, and 380.64 corresponding to I^-, I_2^-, and I_3^-, respectively (theoretical monoisotopic m/z 126.90, 253.81, and 380.71, respectively). The spatial distribution of triiodide (m/z 380.64) shows excellent agreement with the "S" character, as shown in Figure 2b. The distribution of $[M-H]^-$ from citric acid (m/z 191.09, theoretical monoisotopic m/z 191.02) shows the optically invisible diagonal mark drawn on the sample. The imaging experiment was performed using a step size of 25 μm under atmospheric conditions.

Imaging biological samples is one of the most promising applications of IMS. We selected onion epidermis tissue, a classic sample in optical microscopy, to demonstrate the ability of our method to image biological samples with unprecedented spatial resolution at atmospheric pressure using mass spectrometry. This tissue was selected because it contains cells of appropriate sizes (~50 μm width) to be resolved with the current spatial resolution of our system. Figure 3 shows the laser-induced mass spectra in negative and positive ion modes obtained after a 100 μm step of the sample across the laser focal spot. The spectra show the presence of common plant metabolites. The peaks at m/z 179.05,

(34) Schilmiller, A.; Shi, F.; Kim, J.; Charbonneau, A. L.; Holmes, D.; Jones, A. D.; Last, R. L. *Plant J.*, DOI: 10.1111/j.1365-313X.2010.04154.x.

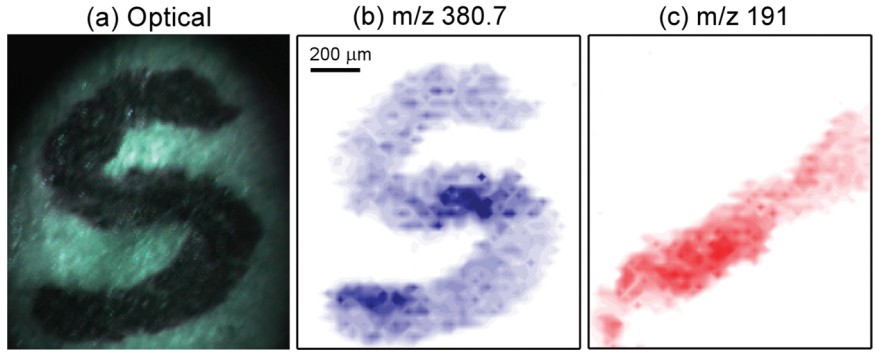

Figure 2. Chemical image of a dye pattern obtained under atmospheric conditions. (a) Optical image of the sample. The "S" character was drawn with iodine/iodide dye. Although not visible, a diagonal line drawn across the "S" with citric acid is also present in the sample. (b) The distribution of triiodide (*m/z* 380.64), which shows an excellent agreement with the "S" character. (c) The distribution of citrate (*m/z* 191.09), invisible in the optical image, shows the diagonal line drawn across the "S" character with citric acid. The step size is 25 μm.

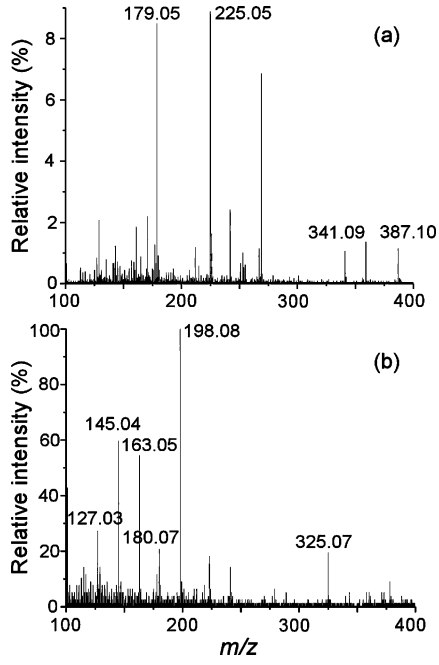

Figure 3. Mass spectra of onion epidermis tissue generated using femtosecond laser desorption ionization. Common plant metabolites were identified. (a) Negative ion mode. The annotated peaks at *m/z* 179.05, 225.05, 341.09, and 387.10 correspond to the $[M-H]^-$ of glucose, $[M+formate]^-$ of glucose, $[M-H]^-$ of sucrose, and $[M+formate]^-$ of sucrose, respectively. (b) Positive ion mode. The annotated peaks at *m/z* 127.03, 145.04, 163.05, 180.07, 198.08, and 325.07 are consistent with $[M+H^+-3H_2O]^+$ of glucose, $[M+H^+-2H_2O]^+$ of glucose, $[M+H^+-H_2O]^+$ of glucose, $[M+NH_4^+-H_2O]^+$ of glucose, $[M+NH_4^+]^+$ of glucose, and $[M+H^+-H_2O]^+$ of sucrose, respectively.

225.05, 341.09, and 387.10 in Figure 3a correspond to the $[M-H]^-$ of glucose (with possible contribution from other isomeric hexoses), $[M+formate]^-$ of glucose, $[M-H]^-$ of sucrose, and $[M+formate]^-$ of sucrose. These assignments were confirmed by coincident retention times and accurate mass measurements from LC/MS analyses of onion extracts (see Metabolite Identification) which detected glucose as a minor constituent (*m/z* 179.0553, theoretical monoisotopic *m/z* 179.0561) and sucrose as an abundant metabolite (*m/z* 341.1078, theor. *m/z* 341.1089). In Figure 3b the peaks at *m/z* 127.03, 145.04, 163.05, 180.07, 198.08, and 325.07 are consistent with $[M+H^+-3H_2O]^+$ of glucose, $[M+H^+-2H_2O]^+$ of glucose, $[M+H^+-H_2O]^+$ of glucose,

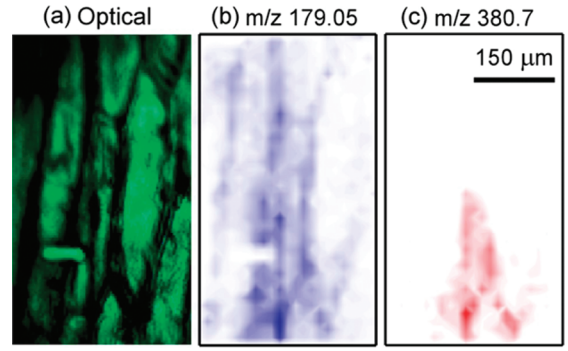

Figure 4. Chemical image of onion epidermis cells obtained under atmospheric conditions in negative ion mode. (a) Optical image (false color) of the tissue analyzed. The lower right region was partially stained with an iodine/iodide dye and appears slightly darker than the rest of the tissue. The horizontal mark was produced by ablating the tissue with the laser to determine the sampling width of the laser spot. (b) Chemical image of the same region showing the spatial distribution of deprotonated glucose (*m/z* 179.06). Note the excellent agreement with the optical image. (c) Chemical image of the same region showing the spatial distribution of triiodide (*m/z* 380.64). The step size for both chemical images was 15 μm.

$[M+NH_4^+-H_2O]^+$ of glucose, $[M+NH_4^+]^+$ of glucose, and $[M+H^+-H_2O]^+$ of sucrose (theor. *m/z* 127.04, 145.05, 163.06, 180.09, 198.10 and 325.11, respectively).

Imaging experiments were performed in the negative ion mode. Given that the width of the tissue cells in our experiments was ~50 μm, a resolution higher than ~20 μm was necessary to resolve individual cells. At these resolutions, obtained by decreasing the step size, only the peaks at *m/z* 179.06 and 225.06 were detected and both showed similar spatial distributions. To enhance chemical contrast, a portion of the sample was stained with an iodine/iodide dye which is commonly used to stain starch. Figure 4a shows the optical image (false color) of the sample. The stained region of the sample appears at the lower right region and is slightly darker than the rest of the tissue. The horizontal mark at the lower left region was intentionally produced by ablating the tissue with the laser. Figure 4b and c corresponds to chemical images obtained using a 15 μm step size. Figure 4 shows the spatial distribution of deprotonated glucose ions (*m/z* 179.06). Note that higher *m/z* 179 regions (darker blue) match the location of the cell walls in the tissue, and thus the glucose ions are probably produced by fragmentation of cellulose from the cell

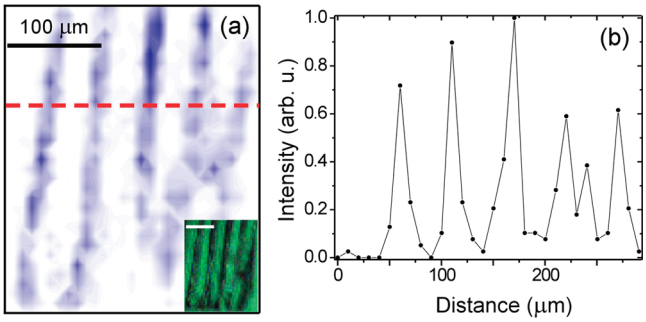

Figure 5. Chemical image of onion epidermis cells demonstrating the highest spatial resolution under atmospheric pressure conditions. (a) Chemical image generated in negative ion mode showing the spatial distribution of *m*/*z* 179 generated by probing the onion epidermis tissue. The inset shows the corresponding optical image. The scale bar in the inset is 100 μm. (b) Intensity distribution of *m*/*z* 179 corresponding to the red dashed line shown in (a). The analysis of several line scans such as the one shown indicated an experimental spatial resolution of ~10 μm.

walls. The ablated region also appears clearly in the chemical image. The spatial distribution of triiodide (*m*/*z* 380.64), from the dye solution, is shown in Figure 4c and agrees well with the location of the stained region.

The single pixel resolution of an experiment (step size) does not necessarily agree with the experimental spatial resolution of an image (the length scale that can be distinguished), which depends also on other factors such as the spatial distribution of analytes in the sample and the signal intensity per pixel.[2] A way to estimate the experimental spatial resolution is by examining a line across a feature of interest and measuring the distance required to move from 20 to 80% of the maximum intensity value of the feature.[35] To estimate the experimental spatial resolution of our system, we recorded another chemical image of onion epidermis using a 10 μm step size. Smaller step sizes compromised reproducibility of signal intensities across the sample in the present configuration of our setup. Figure 5a shows the chemical image of the tissue showing the spatial distribution of *m*/*z* 179 (deprotonated glucose). The inset shows the corresponding optical image (false color). The experimental spatial resolution was calculated as ~10 μm from the analysis of several line scans across the image. An example of such line scans is shown as a red dashed line in Figure 5a and its corresponding intensity profile is shown in Figure 5b. To our knowledge, this is the highest spatial resolution chemical image obtained at AP conditions.

The cell monolayers analyzed previously were completely ablated during the imaging experiment. However, the damage inflicted by the laser on thicker biological samples is superficial and most plant and animal tissue samples can survive the analysis. In vivo chemical imaging experiments are therefore possible with AP fs-LDI IMS.

While the identified peaks in the mass spectra of onionskin epidermis (Figure 3) likely correspond to cellulose fragments, the molecular ion is typically present in the AP fs-LDI mass spectrum of low molecular weight (<400 Da) solid samples of metabolite standards. The $[M-H]^-$ of the analyte is observed for acidic metabolites analyzed in negative ion mode such as in the case of citric acid. Similarly, the $[M+H]^+$ of the analyte is observed for molecules analyzed in positive ion mode such as tyrosine and 2,4-dinitrotoluene (not shown). The ionization of heavier molecules with AP fs-LDI has not been studied thoroughly, but molecular ions of molecules heavier than 400 Da have not been observed so far. As it is also suggested by the mass spectra shown in Figure 3 the ion yield of AP fs-LDI seems to decrease with increasing mass probably due to inefficient ablation for heavier fragments or inefficient transport of ions from the sample surface into the mass spectrometer using the present source configuration.

The limit of detection (LOD) of the method was calculated analyzing a layer of citric acid deposited on the sample holder (see Materials and Sample Preparation). The mass spectra corresponding to ten different laser spots (20 μm diameter) were averaged yielding a signal-to-noise ratio (S/N) of 5:1 for the citrate ion (*m*/*z* 191). Assuming that all the deposited material was ablated from the illuminated area, each laser spot would provide ~500 fmol of citric acid molecules. Other AP IMS techniques including DESI, LAESI, and IR MALDI have limits of detection of a few fmol.[12] Note that in IR MALDI a laser-absorbing matrix present in high concentration resonantly absorbs the laser radiation.[14] In contrast, nonresonant laser-analyte interaction with no matrix occurs in fs-LDI. This difference may explain the higher LOD observed for fs-LDI. Laser desorption experiments have shown to produce a significant amount of neutrals together with ions.[9,12] Therefore, the introduction of a secondary ionization method such as ESI after laser desorption[12,27] is expected to increase the ionization efficiency of fs-LDI. Additional improvements in the sensitivity of AP fs-LDI can be expected by optimizing several of the AP ion source parameters including the potentials on the sample cone, sample holder, and electrode; and the distances between the electrode, sample holder, laser focal spot, and sample cone. No effort was made here to synchronize the ion packets generated by the laser with the pusher pulses in the mass spectrometer. Such synchronization together with the use of an analog-to-digital converter, rather than the time-to-digital electronics in the current detection system offer opportunities to significantly increase the sensitivity and dynamic range of the method.

CONCLUSIONS

A novel IMS approach using near-IR femtosecond laser pulses for direct sample desorption and ionization at AP conditions has been presented. Given that ablation and ionization occur via nonlinear laser-analyte interactions the presence of a laser-absorbing matrix is not required. Consequently, sample preparation and handling are significantly simplified compared to AP MALDI IMS techniques.

In its current level of development AP fs-LDI IMS offers a limited *m*/*z* range (*m*/*z* < 400) and sensitivity compared to other AP IMS techniques. Both figures of merit can be improved by adding a secondary ionization method following laser desorption to improve the ionization efficiency, by optimizing several of the AP ion source parameters to enhance ion collection, and by introducing ion packet-pusher pulse synchronization with new ADC detectors.

In contrast to the established vacuum IMS techniques MALDI and SIMS, AP fs-LDI IMS allows the analysis of biological samples

(35) Colliver, T. L.; Brummel, C. L.; Pacholski, M. L.; Swanek, F. D.; Ewing, A. G.; Winograd, N. *Anal. Chem.* **1997**, *69*, 2225–2231.

in their natural state. Improvements in the sensitivity of the setup, as described before, will minimize damage to the sample and make in vivo investigations more feasible.

While no AP IMS technique can compete with SIMS imaging in terms of spatial resolution yet, the 10 μm spatial resolution for biological tissue demonstrated here with AP fs-LDI IMS represents an improvement over other AP IMS techniques and a step toward mass spectrometric chemical imaging at the cellular level. Efforts to increase resolution will also require improvements in the sensitivity in order to maintain an acceptable S/N. The resolution of the system could then be improved by reducing the laser focal spot diameter and the step size. The laser pulses used here can be focused to $\sim$1 μm using a higher magnification objective. In theory, the smallest possible focal spot diameter would be determined by the diffraction limit $\sim\lambda/2$, 400 nm in this case. Because the ionization and ablation processes produced by focused femtosecond pulses are highly nonlinear, it is conceivable that subdiffraction-limit focal spot diameters could be ablated. This would allow, for instance, imaging subcellular structures.

ACKNOWLEDGMENT

We gratefully acknowledge funding for this research from the National Science Foundation grant SGER-CHE-0647901. We thank Prof. Gavin E. Reid, Dr. Scott A. Smith, and Prof. Vadim V. Lozovoy for useful suggestions.

Received for review November 18, 2009. Accepted February 24, 2010.

AC9026466